SIAM J. APPL. MATH.
Vol. 73, No. 2, pp. 1038–1057

CONTROLLING THE UNSTEADY ANALOGUE OF SADDLE STAGNATION POINTS*

SANJEEVA BALASURIYA† AND KATHRIN PADBERG-GEHLE‡

Abstract. It is well known that saddle stagnation points are crucial flow organizers in steady (autonomous) flows due to their accompanying stable and unstable manifolds. These have been extensively investigated experimentally, numerically, and theoretically in situations related to macro- and micromixers in order to either restrict or enhance mixing. Saddle points are also important players in the dynamics of mechanical oscillators, in which such points and their associated invariant manifolds form boundaries of basins of attraction corresponding to qualitatively different types of behavior. The entity analogous to a saddle point in an unsteady (nonautonomous) flow is a time-varying hyperbolic trajectory with accompanying stable and unstable manifolds which move in time. Within the context of nearly steady flows, the unsteady velocity perturbation required to ensure that such a hyperbolic (saddle) trajectory follows a specified trajectory in space is derived and shown to be equivalent to that which can be obtained via a heuristic approach. An expression for the error in the hyperbolic trajectory's motion is also derived. This provides a new tool for the control of both fluid transport and mechanical oscillators. The method is applied to two examples—a four-roll mill and a Duffing oscillator—and the performance of the control strategy is shown to be excellent in both instances.

Key words. stagnation point, hyperbolic trajectory, nonautonomous flows, saddle point, flow control, oscillator control

AMS subject classifications. 34H05, 76B72, 34A26, 37N10, 70Q05, 34E10

DOI. 10.1137/120886042

1. Introduction.

In steady two-dimensional fluid flows, saddle stagnation points have long been recognized as being crucial flow organizers. Their stable and unstable manifolds separate the flow regime into regions of fluid which do not mix. Analysis of saddle stagnation points is well established in fluid applications ranging from groundwater modeling [29, 46], macro- and micromixing devices [17, 2, 6, 50, 42, 21], and oceanographic flows [48, 3, 36, 11, 9, 40]. The analogous entity in unsteady flows is that of a hyperbolic trajectory, a specific type of time-varying fluid parcel trajectory which possesses time-varying stable and unstable manifolds, whose locations govern fluid transport; cf. [38]. These cannot be identified by examining points in the flow at which fluid particles are instantaneously at rest (cf. [20]), as is easily rationalized by the thought experiment of observing a steady saddle stagnation point in a moving frame. The flow-regulating trajectory is a time-varying entity in this moving frame and does not correspond to a location at which the fluid velocity is zero. A theoretical definition for hyperbolic trajectories can be given in terms of exponential dichotomies [10, 51, 41, 32, 35, 7, 5], but such a definition is generally difficult to use to locate hyperbolic trajectories even for a specified unsteady Eulerian velocity field. While this hinders the analysis and numerical determination of hyperbolic trajectories, there is

*Received by the editors July 26, 2012; accepted for publication (in revised form) February 11, 2013; published electronically April 23, 2013.
http://www.siam.org/journals/siap/73-2/88604.html
†Department of Mathematics, Connecticut College, New London, CT 06320, and School of Mathematical Sciences, University of Adelaide, SA 5005, Australia (sanjeevabalasuriya@yahoo.com). This author's work was supported by the Simons Foundation via a Collaboration grant for Mathematicians.
‡Institute of Scientific Computing, Technische Universität Dresden, D-01062 Dresden, Germany (kathrin.padberg@tu-dresden.de).

strong interest in *controlling* their location (see, e.g., [2, 21, 42]), in order to control (either enhance or decrease) fluid mixing.

While the time-variation of hyperbolic trajectories has implications for fluid transport when considering Lagrangian particle motion in fluid mechanics as described above, it is equally important in other applications in which the phase space is not necessarily physical space. Classical examples here include the pendulum and Duffing equations with time-dependent forcing [18, 28, 27, 25, 45, 34], in which a study of potential chaotic motion is related to intersections of stable and unstable manifolds *of hyperbolic trajectories* in the position-velocity phase space. The eventual behavior of such an oscillator system is highly sensitive to the choice of initial condition near such hyperbolic trajectories, since the associated stable and unstable manifolds demarcate regions which have different fates. Indeed, these manifolds form time-varying boundaries of basins of attraction and are of paramount importance in ideas on "controlling chaos" [33, 15, 28, 8] and in defining stability boundaries of biological and mechanical systems [1, 14, 39]. Time-varying (saddle-like) hyperbolic trajectories are therefore the locations of the intersections of these basin boundaries, and controlling this location in position-velocity space is one part of controlling the long-term behavior of mechanical oscillator systems.

There have been few studies which give insight into how to control such hyperbolic trajectories. One approach [7] provides a bound on a time-dependent perturbation on a steady flow with an attracting stagnation point, which ensures that its unsteady version remains within a specified safety region. Being for nodes rather than saddles, this has lesser applicability for flow separators and transport. Another study addresses a control strategy to push fluid particles which are near unsteady saddles towards them [51]. The approach taken in [51] applies the classical concept of chaos control—following the pioneering work by Ott, Grebogi, and Yorke (OGY) [33]—to stabilize a hyperbolic trajectory. The original OGY method aims at controlling chaotic trajectories onto a neighboring unstable periodic orbit by means of the linearized Poincaré map, thereby stabilizing the periodic dynamics. A related approach based on a continuous feedback control has been proposed by Pyragas [37].

The concept of controlling chaos has received considerable scientific interest in the past 20 years; see, e.g., [16] for a review of the vast literature. Our article offers a different perspective: the explicit determination of the perturbing unsteady vector field needed to ensure that a hyperbolic trajectory follows a *specified* trajectory in space. Notably the target trajectory is *not* stabilized but remains of saddle type, having crucial implications for transport and mixing. The control strategy is derived in section 2. In section 3 we show that an equivalent representation is possible via a quick heuristic argument, and we also give an error bound on how closely the actual hyperbolic trajectory shadows the desired motion as a result of our control. In section 4, we show how our control strategy can be adapted for situations which are slightly different from that discussed in sections 2 and 3. A fluid dynamics example based on the paradigmatic four-roll mill [6, 31, 52, 49, 26, 23, 47, 22, 43] is studied in section 5, in which the idea is to control the position of a hyperbolic trajectory in the apparatus to be exactly at the location of a droplet for which an extensional deformation is to be obtained. As an oscillator example, the double-well Duffing oscillator [18, 28, 27, 25, 45, 30] is examined in section 6. Its hyperbolic trajectory can be controlled to be at specified time-varying locations via suitably modifying an applied forcing, thereby positioning the location of the intersection of basins of attraction at any desired location.

2. Control strategy. We wish to control the location of hyperbolic trajectories in the system

$$\dot{\mathbf{x}} = \mathbf{v}(\mathbf{x}, t, \varepsilon) = \mathbf{v}_0(\mathbf{x}) + \varepsilon\, \mathbf{v}_1(\mathbf{x}, t), \tag{2.1}$$

in which $\mathbf{x}$ is two-dimensional, ε is a small parameter, and the vector field $\mathbf{v}$ is smooth. The unsteady velocity $\mathbf{v}_1$ is to be considered the control, which is to be determined in order to move a saddle stagnation point of the $\varepsilon = 0$ system to a hyperbolic trajectory which exhibits a desired time-varying motion. As we discuss in section 4, the method we develop is easily adaptable to slightly different situations, such as when the unperturbed ($\varepsilon = 0$) flow is itself unsteady, or when a control velocity is to be added to an uncontrolled flow which has the form (2.1).

In the fluid dynamics situation, the vector field $\mathbf{v}$ is precisely the Eulerian velocity, whereas it would be a more general function for an oscillator system. More details on these technical smoothness assumptions are available [4]; in brief, $\mathbf{v}_0$ needs to be C^2, and $\mathbf{v}_1$ to be C^2 in space and C^1 in time, with $\mathbf{v}_1$ and its spatial derivative bounded in time. The steady $\varepsilon = 0$ flow,

$$\dot{\mathbf{x}} = \mathbf{v}_0(\mathbf{x}), \tag{2.2}$$

is assumed to possess a saddle (hyperbolic) stagnation (fixed) point at $\mathbf{a}$ in that (i) $\mathbf{v}_0(\mathbf{a}) = \mathbf{0}$, and (ii) the Jacobian matrix $D\mathbf{v}_0$ when evaluated at $\mathbf{a}$ has real eigenvalues $\lambda_u > 0$ and $\lambda_s < 0$, with corresponding eigenvectors $\mathbf{u}$ and $\mathbf{s}$. In what follows, these eigenvectors are chosen to be of unit length and in the direction of flow along the corresponding one-dimensional stable and unstable manifolds of $\mathbf{a}$; see Figure 1.

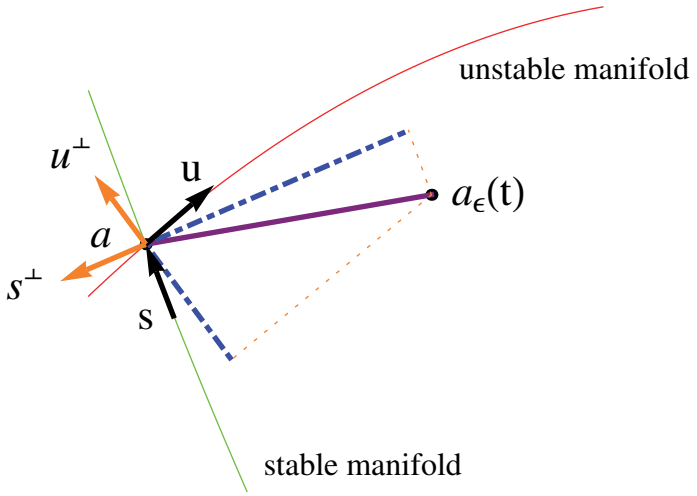

FIG. 1. *Locating the hyperbolic trajectory in a time-slice t. The components of the vector* $\mathbf{a}_\varepsilon(t) - \mathbf{a}$ *in the directions* $\mathbf{u}^\perp$ *and* $\mathbf{s}^\perp$ *are indicated by the dot-dashed lines.*

When $\varepsilon \neq 0$, the flow (2.1) is unsteady (nonautonomous). In this situation, it makes sense to view (2.1) in the form $\dot{\mathbf{x}} = \mathbf{v}(\mathbf{x}, t, \varepsilon)$, $\dot{t} = 1$, in order to make the system autonomous. When considering this *augmented system* at $\varepsilon = 0$, the saddle stagnation point becomes a straight line hyperbolic trajectory with two-dimensional stable and unstable manifolds, as illustrated in Figure 2. Trajectories on these manifolds (labeled ts and tu) decay towards the hyperbolic trajectory $(\mathbf{a}, t)$ in forwards/backwards time,

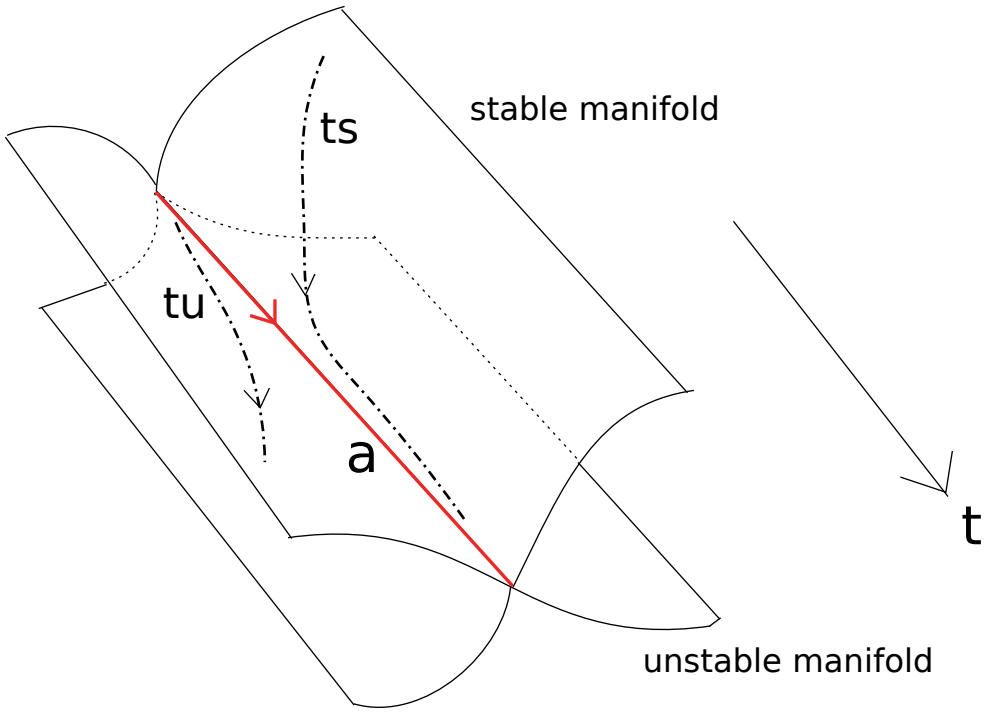

FIG. 2. *Hyperbolic trajectory* $(\mathbf{a}, t)$ *(i.e., saddle) in* $(\mathbf{x}, t)$ *space.*

and these manifolds separate fluid regions which do not mix. When $\varepsilon \neq 0$, the solution $(\mathbf{a}, t)$ of (2.2) perturbs to a nearby solution $(\mathbf{a}_\varepsilon(t), t)$ of (2.1), which turns out to continue to be hyperbolic in the following sense. In nonautonomous systems such as (2.1), hyperbolicity needs to be defined in terms of *exponential dichotomies* [10, 41, 32, 35] of the associated variational equation

$$\dot{\mathbf{y}} = \left[D\mathbf{v}_0\left(\mathbf{a}_\varepsilon(t)\right) + \varepsilon D\mathbf{v}_1\left(\mathbf{a}_\varepsilon(t), t\right)\right]\mathbf{y}\,. \tag{2.3}$$

When $\varepsilon = 0$, (2.3) is the variational equation associated with (2.2) at the solution $\mathbf{x} = \mathbf{a}$. As long as the perturbation $\mathbf{v}_1$ is sufficiently smooth in $\mathbf{x}$ and bounded in t, and $|\varepsilon|$ is sufficiently small, there exists a trajectory $\mathbf{a}_\varepsilon(t)$ of (2.1) such that (2.3) continues to satisfy exponential dichotomy conditions when $\varepsilon \neq 0$ [10, p. 34], [53, p. 279], [51]. The new hyperbolic trajectory $(\mathbf{a}_\varepsilon(t), t)$ is a "wobbled" version of $(\mathbf{a}, t)$. The retention of stable and unstable manifolds also follows directly from the persistence of exponential dichotomies, since these manifolds are locally represented using the projection matrices guaranteed by exponential dichotomies [10, 53]. These manifolds are no longer uniform in t and now form *time-varying* flow separators. When taking a time-slice t of the perturbed version of Figure 2, the point $\mathbf{a}$ is now at a nearby location $\mathbf{a}_\varepsilon(t)$, as indicated in Figure 1.

Given $\mathbf{v}_1(\mathbf{x}, t)$, recent work [4] enables locating $\mathbf{a}_\varepsilon(t)$ in terms of the unit vector directions $\mathbf{s}^\perp$ and $\mathbf{u}^\perp$, which are obtained by rotating $\mathbf{s}$ and $\mathbf{u}$ by $\pi/2$ counterclockwise. The analysis uses Melnikov theory from a geometric perspective to locate the perturbed stable and unstable manifolds at a general time-instance and a general location on the manifold, after which a limiting procedure of going along the manifolds towards the former saddle point is used [4]. The $\mathcal{O}(\varepsilon)$ projections of $\mathbf{a}_\varepsilon(t) - \mathbf{a}$

in the directions $\mathbf{u}^\perp$ and $\mathbf{s}^\perp$, which are indicated with the dot-dashed lines in Figure 1, turn out to be [4]

$$\left.\begin{aligned} \alpha_u(t) &:= \mathcal{L}_\tau \left\{ \mathbf{v}_1 \left(\mathbf{a}, t-\tau\right) \cdot \mathbf{u}^\perp \right\} \left(-\lambda_s\right), \\ \alpha_s(t) &:= -\mathcal{L}_\tau \left\{ \mathbf{v}_1 \left(\mathbf{a}, t+\tau\right) \cdot \mathbf{s}^\perp \right\} \left(\lambda_u\right), \end{aligned}\right\} \tag{2.4}$$

where $\mathcal{L}_\tau$ represents the Laplace transform with respect to the variable τ. A simple geometric argument enables $\mathbf{a}_\varepsilon(t)$ to be expressed in the $(\mathbf{u}^\perp, \mathbf{u})$ orthogonal basis by [4]

$$\mathbf{a}_\varepsilon(t) = \mathbf{a} + \varepsilon \left[\alpha_u(t)\, \mathbf{u}^\perp + \frac{\alpha_u(t)\, (\mathbf{u}\cdot\mathbf{s}) - \alpha_s(t)}{\mathbf{u}^\perp \cdot \mathbf{s}}\, \mathbf{u} \right] + \mathcal{O}(\varepsilon^2)\,. \tag{2.5}$$

The basis $(\mathbf{s}^\perp, \mathbf{s})$ could be used alternatively in (2.5), by performing the interchange $\mathbf{u} \leftrightarrow \mathbf{s}$ throughout in (2.5). While this result permits locating $\mathbf{a}_\varepsilon(t)$ for a given $\mathbf{v}_1$, the reverse question is now posed: Can one figure out the velocity perturbation $\mathbf{v}_1$ that is needed for the hyperbolic trajectory to follow a *specified* $\mathbf{a}_\varepsilon(t)$, which is $\mathcal{O}(\varepsilon)$-close to $\mathbf{a}$?

To solve this control problem, let ε be small and fixed. For a given differentiable hyperbolic trajectory $\mathbf{a}_\varepsilon(t)$, define

$$\left.\begin{aligned} \tilde{\alpha_u}(t) &:= \frac{(\mathbf{a}_\varepsilon(t) - \mathbf{a}) \cdot \mathbf{u}^\perp}{\varepsilon}, \\ \tilde{\alpha_s}(t) &:= \frac{(\mathbf{a}_\varepsilon(t) - \mathbf{a}) \cdot \mathbf{s}^\perp}{\varepsilon}, \end{aligned}\right\} \tag{2.6}$$

$\mathcal{O}(1)$ quantities which are proxies for $\alpha_{u,s}(t)$. From the first equation in (2.4),

$$\begin{aligned} \alpha_u(t) &= \int_0^\infty \mathbf{v}_1(\mathbf{a}, t-\tau) \cdot \mathbf{u}^\perp e^{-(-\lambda_s)\tau}\, \mathrm{d}\tau \\ &= -\int_t^{-\infty} \left(\mathbf{v}_1(\mathbf{a}, \mu) \cdot \mathbf{u}^\perp\right) e^{\lambda_s(t-\mu)} \mathrm{d}\mu \\ &= e^{\lambda_s t} \int_{-\infty}^t \left(\mathbf{v}_1(\mathbf{a}, \mu) \cdot \mathbf{u}^\perp\right) e^{-\lambda_s \mu} \mathrm{d}\mu\,, \end{aligned}$$

and thus

$$\alpha_u(t) e^{-\lambda_s t} = \int_{-\infty}^t \left(\mathbf{v}_1(\mathbf{a}, \mu) \cdot \mathbf{u}^\perp\right) e^{-\lambda_s \mu} \mathrm{d}\mu\,. \tag{2.7}$$

By differentiating, we obtain $(\alpha_u(t) e^{-\lambda_s t})' = (\mathbf{v}_1(\mathbf{a}, t) \cdot \mathbf{u}^\perp) e^{-\lambda_s t}$, which upon rearranging yields

$$\alpha_u'(t) - \lambda_s \alpha_u(t) = \mathbf{v}_1(\mathbf{a}, t) \cdot \mathbf{u}^\perp,$$

and thus the projection of $\mathbf{v}_1$ in the direction of $\mathbf{u}^\perp$ is given by the left-hand side above. Since α_u is within $\mathcal{O}(\varepsilon)$ of $\tilde{\alpha}_u$, and also α_u' is within $\mathcal{O}(\varepsilon)$ of $\tilde{\alpha}_u'$, the required projection of $\mathbf{v}_1$ can be determined to $\mathcal{O}(\varepsilon)$ by

$$\mathbf{v}_1(\mathbf{a}, t) \cdot \mathbf{u}^\perp = \tilde{\alpha}_u'(t) - \lambda_s \tilde{\alpha}_u(t) + \mathcal{O}(\varepsilon). \tag{2.8}$$

A similar argument from the second equation in (2.4) leads to

$$\mathbf{v}_1(\mathbf{a},t)\cdot\mathbf{s}^{\perp} = \tilde{\alpha}_s'(t) - \lambda_u\tilde{\alpha}_s(t) + \mathcal{O}(\varepsilon). \tag{2.9}$$

Now, since the components of $\mathbf{v}_1$ are known in two independent directions by (2.8) and (2.9), it is possible to write $\mathbf{v}_1$ in terms of the orthogonal system $(\mathbf{u}^{\perp},\mathbf{u})$ by the same process as (2.5). The required unsteady perturbation in the Eulerian velocity field, correct to $\mathcal{O}(\varepsilon)$, is

$$\mathbf{v}_1(\mathbf{a},t) = \left[\beta_u(t)\mathbf{u}^{\perp} + \frac{\beta_u(t)\,(\mathbf{u}\cdot\mathbf{s}) - \beta_s(t)}{\mathbf{u}^{\perp}\cdot\mathbf{s}}\,\mathbf{u}\right], \tag{2.10}$$

where the β's are the components in the $\mathbf{u}^{\perp}$ and $\mathbf{s}^{\perp}$ directions as derived in (2.8) and (2.9), i.e.,

$$\left.\begin{aligned}\beta_u(t) &:= \tilde{\alpha}_u'(t) - \lambda_s\tilde{\alpha}_u(t),\\ \beta_s(t) &:= \tilde{\alpha}_s'(t) - \lambda_u\tilde{\alpha}_s(t),\end{aligned}\right\} \tag{2.11}$$

in which $\tilde{\alpha}_{u,s}(t)$ is defined in terms of the required trajectory $\mathbf{a}_\varepsilon(t)$ in (2.6).

3. Control strategy via formal expansion. The control strategy derived in the previous section requires computation of the unit vectors $\mathbf{u}$, $\mathbf{s}$, $\mathbf{u}^{\perp}$, and $\mathbf{s}^{\perp}$, followed by evaluation of the quantities $\tilde{\alpha}_{u,s}$ and $\beta_{u,s}$, before the control equation (2.10) can be used to evaluate the required velocity $\mathbf{v}_1(\mathbf{a},t)$. It turns out that a much easier representation of (2.10) is possible, which can be derived using a heuristic approach. Using this approach, it is also possible to quantify the expected error while using our control strategy in attempting to keep a hyperbolic trajectory at a desired location $\mathbf{a}_\varepsilon(t)$.

We wish to control a hyperbolic trajectory $\mathbf{a}_\varepsilon(t)$ of (2.1) which is $\mathcal{O}(\varepsilon)$-close to the hyperbolic fixed point $\mathbf{a}$ of (2.2) for all time. Suppose we formally Taylor expand

$$\mathbf{a}_\varepsilon(t) = \mathbf{a} + \varepsilon\mathbf{x}_1(t) + \varepsilon^2\left[\mathbf{x}_2(t) + \mathcal{O}(\varepsilon)\right] =: \mathbf{a} + \varepsilon\mathbf{x}_1(t) + \mathbf{E}(t,\varepsilon), \tag{3.1}$$

which defines the error $\mathbf{E}(t,\varepsilon)$ in approximating $\mathbf{a}_\varepsilon(t)$ with $\mathbf{a}+\varepsilon\mathbf{x}_1(t)$. Given any $\mathbf{a}_\varepsilon(t)$ which is sufficiently smooth in ε and which satisfies $\mathbf{a}_0(t)=\mathbf{a}$, we can think of *obtaining* $\mathbf{x}_1(t)$ from this by

$$\mathbf{x}_1(t) = \left.\frac{\partial\mathbf{a}_\varepsilon(t)}{\partial\varepsilon}\right|_{\varepsilon=0}$$

for subsequent use in our control strategy. The problem now is to determine the perturbing velocity $\mathbf{v}_1$ associated with $\mathbf{x}_1(t)$. Substituting (3.1) into (2.1) for $\mathbf{x}$ gives the expression

$$\begin{aligned}\varepsilon\dot{\mathbf{x}}_1(t) + \varepsilon^2\dot{\mathbf{x}}_2(t) + \cdots = \mathbf{v}_0\big(\mathbf{a} + \varepsilon\mathbf{x}_1(t) + \varepsilon^2\mathbf{x}_2(t) + \cdots\big)\\ + \varepsilon\mathbf{v}_1\left(\mathbf{a} + \varepsilon\mathbf{x}_1(t) + \varepsilon^2\mathbf{x}_2(t) + \cdots, t\right).\end{aligned} \tag{3.2}$$

Formally Taylor expanding (3.2) in ε and noting that $\mathbf{v}_0(\mathbf{a}) = \mathbf{0}$, we see that the $\mathcal{O}(\varepsilon^0)$ term vanishes. Rearranging the $\mathcal{O}(\varepsilon)$ term gives us the expression

$$\mathbf{v}_1(\mathbf{a},t) = \dot{\mathbf{x}}_1 - D\mathbf{v}_0(\mathbf{a})\,\mathbf{x}_1(t), \tag{3.3}$$

and hence, knowing $\mathbf{x}_1$ and the linearization matrix for the steady flow around the saddle stagnation point $\mathbf{a}$, we can directly compute the $\mathbf{v}_1$ needed. It must be emphasized that this approach is purely formal. On the other hand, it is possible via

tedious but straightforward calculations to verify that the expression (3.3) is *identical* to the control strategy (2.10) derived previously. In other words, our work in section 2, building on previous analysis [4], nicely shores up this formal expansion process. Thus, from an operational viewpoint, the heuristically derived (3.3) can be used directly to solve the relevant control problem. We verify this equivalence in the examples to follow.

Next, we estimate the error $\mathbf{E}(t,\varepsilon)$ in the hyperbolic trajectory associated with using a control velocity (3.3). This is accomplished by examining the $\mathcal{O}(\varepsilon^2)$ terms in (3.2), which leads to the differential equation

$$\dot{\mathbf{x}}_2(t) = D\mathbf{v}_0(\mathbf{a})\,\mathbf{x}_2(t) + \frac{1}{2}\mathbf{x}_1^T(t)D^2\mathbf{v}_0(\mathbf{a})\,\mathbf{x}_1(t) + D\mathbf{v}_1(\mathbf{a})\,\mathbf{x}_1(t),$$

whose solution is

$$\mathbf{x}_2(t) = e^{D\mathbf{v}_0(\mathbf{a})t}\int_0^t e^{-D\mathbf{v}_0(\mathbf{a})\tau}\left[\frac{1}{2}\mathbf{x}_1^T(\tau)D^2\mathbf{v}_0(\mathbf{a})\,\mathbf{x}_1(\tau) + D\mathbf{v}_1(\mathbf{a})\,\mathbf{x}_1(\tau)\right]\mathrm{d}\tau.$$

In order to evaluate $\mathbf{x}_2$, we note that we need the derivative of $\mathbf{v}_1$ at $\mathbf{a}$, which has *not* been specified in the control strategy (3.3). Unsurprisingly, the behavior of $\mathbf{v}_1$ in the vicinity of $\mathbf{a}$ has an influence on the error. Thus from (3.1) the required error is

(3.4)
$$\mathbf{E}(t,\varepsilon) = \varepsilon^2\left[e^{D\mathbf{v}_0(\mathbf{a})t}\int_0^t e^{-D\mathbf{v}_0(\mathbf{a})\tau}\left[\frac{1}{2}\mathbf{x}_1^T(\tau)D^2\mathbf{v}_0(\mathbf{a})\,\mathbf{x}_1(\tau)+D\mathbf{v}_1(\mathbf{a})\,\mathbf{x}_1(\tau)\right]\mathrm{d}\tau+\mathcal{O}(\varepsilon)\right].$$

If the integral above is zero, we see that $\mathbf{E}(t,\varepsilon) = \mathcal{O}(\varepsilon^3)$, and if so, the above computation would need to be extended to higher order to quantify the error. On the other hand, if the integral is nonzero, a bound for the error can be given. Then for small enough ε we have

(3.5)
$$|\mathbf{E}(t,\varepsilon)| \le \varepsilon^2\left|e^{D\mathbf{v}_0(\mathbf{a})t}\int_0^t e^{-D\mathbf{v}_0(\mathbf{a})\tau}\left[\frac{1}{2}\mathbf{x}_1^T(\tau)D^2\mathbf{v}_0(\mathbf{a})\,\mathbf{x}_1(\tau) + D\mathbf{v}_1(\mathbf{a})\,\mathbf{x}_1(\tau)\right]\mathrm{d}\tau\right|.$$

We assume that $\mathbf{x}_1(t)$ is bounded for $t\in\mathbb{R}$ and define

$$c = \left\|\left[D\mathbf{v}_0(\mathbf{a})\right]^{-1}\right\| \sup_{t\in\mathbb{R}}\left|\frac{1}{2}\mathbf{x}_1^T(\tau)D^2\mathbf{v}_0(\mathbf{a})\,\mathbf{x}_1(\tau) + D\mathbf{v}_1(\mathbf{a})\,\mathbf{x}_1(\tau)\right|, \tag{3.6}$$

where $\|\cdot\|$ is the spectral norm of a 2×2 matrix. Now, since the eigenvalues of $D\mathbf{v}_0(\mathbf{a})$ satisfy $\lambda_s < 0 < \lambda_u$, its determinant $\lambda_s\lambda_u < 0$, and it is invertible. Thus, the matrix norm in (3.6) is well-defined. Moreover, under our assumed condition that the integral in (3.5) is nonzero, the supremum in (3.6) will yield a nonzero term, and thus $c > 0$. Pulling out the bound $c/\left\|\left[D\mathbf{v}_0(\mathbf{a})\right]^{-1}\right\|$ from the integral in (3.5) and integrating, we get

$$\begin{aligned}|\mathbf{E}(t,\varepsilon)| &\le \varepsilon^2\frac{c}{\left\|\left[D\mathbf{v}_0(\mathbf{a})\right]^{-1}\right\|}\left\|e^{D\mathbf{v}_0(\mathbf{a})t}\left[-D\mathbf{v}_0(\mathbf{a})\right]^{-1}\left(e^{-D\mathbf{v}_0(\mathbf{a})t}-I\right)\right\| \\ &\le \varepsilon^2 c\left\|e^{D\mathbf{v}_0(\mathbf{a})t}-I\right\|, \end{aligned} \tag{3.7}$$

where I is the identity matrix and standard commutative and submultiplicative properties have been used in the matrix manipulations. Thus, the growth rate of the error term with respect to t is quantified by the term $\left\|e^{D\mathbf{v}_0(\mathbf{a}t)t}-I\right\|$ in (3.7), as long as the integral in (3.4) is nonzero.

4. Extension of control strategy to different situations. The preceding two sections have outlined the condition on the control velocity $\mathbf{v}_1$ such that the system $\dot{\mathbf{x}} = \mathbf{v}_0(\mathbf{x}) + \varepsilon \mathbf{v}_1(\mathbf{x}, t)$ possesses a hyperbolic trajectory that follows a specified trajectory $\mathbf{a}_\varepsilon(t)$ that is $\mathcal{O}(\varepsilon)$-close to a known saddle point $\mathbf{a}$ of the $\varepsilon = 0$ system. The method outlined can in fact be extended to two slightly different situations with hardly any effort.

Situation 1. Suppose that the unperturbed flow were itself nonautonomous:

$$\dot{\mathbf{x}} = \mathbf{v}_0(\mathbf{x}, t) + \varepsilon \mathbf{v}_1(\mathbf{x}, t). \tag{4.1}$$

Suppose we know a hyperbolic trajectory $\mathbf{a}_0(t)$ of (4.1) when $\varepsilon = 0$. In this case, unlike in the main problem discussed so far, the unperturbed hyperbolic trajectory is itself time-varying. Now suppose that we need to determine $\mathbf{v}_1$ in order to move this hyperbolic trajectory to a location $\mathbf{a}_\varepsilon(t)$ which is $\mathcal{O}(\varepsilon)$-close to $\mathbf{a}_0(t)$. Now, the theory discussed previously applies to this situation with hardly any difference. The hyperbolicity of the unperturbed trajectory would need to be expressed in terms of exponential dichotomies [10, 35, 32], and once again, the persistence of exponential dichotomies under perturbations [10, 53, 51] ensures that the system (4.1) possesses a nearby hyperbolic trajectory $\mathbf{a}_\varepsilon(t)$ as long as sufficient smoothness and boundedness of $\mathbf{v}_1$ is present. Thus, the results upon which section 2 are premised [4] extend to this situation as well. This is also easily seen by the modifications needed to the formal calculations in section 3: in order to achieve the hyperbolic trajectory $\mathbf{a}_\varepsilon(t) = \mathbf{a}_0(t) + \varepsilon \mathbf{x}_1(t)$ the required condition would simply be

$$\mathbf{v}_1(\mathbf{a}_0(t), t) = \dot{\mathbf{x}}_1(t) - D\mathbf{v}_0(\mathbf{a}_0(t))\, \mathbf{x}_1(t). \tag{4.2}$$

Applying this more general result immediately suffers difficulties, since we would need to know the hyperbolic trajectory $\mathbf{a}_0(t)$ of a *nonautonomous* situation. Such explicit examples are not readily available in the literature, except in the following situations. The easiest way to come up with such an example is to think of $\mathbf{v}_0(\mathbf{x}, t)$ as arising from examining a steady saddle point situation from a frame moving at a constant speed, in which case the hyperbolic trajectory would simply be the saddle point which moves at a constant velocity. Additional examples related to nonlinear transformations applied to steady flows are known [5], but all these are somewhat artificial, and hence the usefulness of the control strategy in the more general Situation 1 is not compelling.

Situation 2. Suppose instead that the unperturbed flow is steady, but that the perturbation term includes both a known velocity and the required control. That is, consider

$$\dot{\mathbf{x}} = \mathbf{v}_0(\mathbf{x}) + \varepsilon \left[\mathbf{v}_1(\mathbf{x}, t) + \mathbf{c}(\mathbf{x}, t)\right], \tag{4.3}$$

in which $\mathbf{v}_0$ and $\mathbf{v}_1$ are known, and that $\mathbf{a}$ is a saddle fixed point of the $\varepsilon = 0$ flow above. The idea is to determine the control $\mathbf{c}$, which moves the saddle fixed point to a nearby hyperbolic trajectory $\mathbf{a}_\varepsilon(t) = \mathbf{a} + \varepsilon \mathbf{x}_1(t) + \mathcal{O}(\varepsilon^2)$. Now, had there not been an additional known perturbation velocity $\mathbf{v}_1$ present, the required control would be exactly that which has been derived in sections 2 and 3: it needs to satisfy $\mathbf{c}(\mathbf{a}, t) = \dot{\mathbf{x}}_1(t) - D\mathbf{v}_0(\mathbf{a})\, \mathbf{x}_1(t)$ as given in (3.3). The presence of the extra term in (4.3) is easily dealt with by imposing the condition

$$\mathbf{c}(\mathbf{a}, t) = \dot{\mathbf{x}}_1(t) - D\mathbf{v}_0(\mathbf{a})\, \mathbf{x}_1(t) - \mathbf{v}_1(\mathbf{a}, t), \tag{4.4}$$

which ensures that the entire $\mathcal{O}(\varepsilon)$ term satisfies the required condition. The control condition (4.4) will ensure that the hyperbolic trajectory of (4.3) follows the required

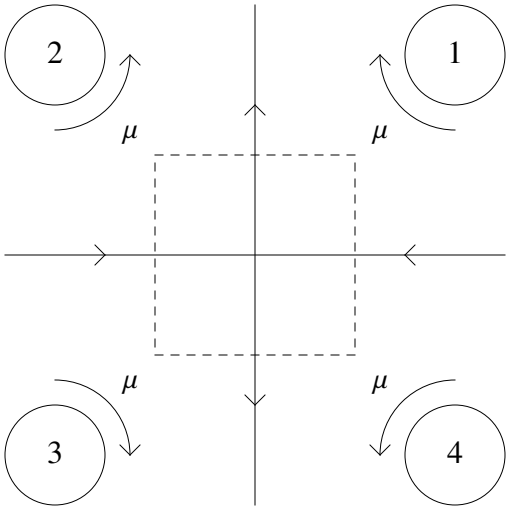

FIG. 3. *The purely straining four-roll mill configuration.*

path to $\mathcal{O}(\varepsilon)$. Thus, this ostensibly more complicated situation is in reality no different from the one we have focussed on.

The situation we address in this article—a steady flow with a saddle point which we require to move to a given nearby time-varying location—therefore incorporates Situations 1 and 2 above.

5. Four-roll mill. As our first example to demonstrate the application of our control strategy, we choose a classical fluidic device conceptualized by Taylor [44] for manipulating deformations of drops in a four-roll mill configuration, as shown in Figure 3. The drop is at the central part of the apparatus (shown by the dashed box), and if the rollers are turned at constant angular velocity μ symmetrically as shown in Figure 3, the central point is a saddle stagnation point. A drop positioned there will be deformed according to the stable and unstable manifolds, and will thus lengthen in the y-direction while shortening in the x-direction. By varying the roller speeds, it is possible to obtain a combination of such purely straining flow with rotational motion at the origin, providing a mechanism for different forms of drop deformation [6, 31, 52, 49, 26, 23, 47, 22, 43]. A major difficulty in such four-roll mills is maintaining a particle precisely at the point of interest, particularly under unsteady rotation protocols.

Here, a specific situation in which one has a time-dependent perturbation of the purely straining flow in Figure 3 is considered. Such would arise if the rollers were rotated at angular velocities $(-1)^i\mu + \varepsilon\mu_i(t)$, in which $|\varepsilon| \ll 1$ and $i = 1, 2, 3, 4$ represent each of the rollers. This results in an unsteady velocity perturbation at the origin, and the theory of this article can be used to determine what this should be to maintain the hyperbolic trajectory at a specified time-varying location near the origin. For a given drop which is seen to move around near the origin, this information can be fed into a control strategy which causes a time-varying velocity perturbation at the origin which then ensures that the drop is exactly at a hyperbolic trajectory. This procedure will ensure that the drop undergoes the straining motion at a saddle-like

hyperbolic trajectory, as opposed to being swept away into one of the quadrants.

Suppose that the unperturbed situation (as in Figure 3) were given by

$$\left.\begin{aligned} \dot{x} &= -\gamma x, \\ \dot{y} &= \gamma y, \end{aligned}\right\} \tag{5.1}$$

where $\gamma > 0$ is proportional to the steady angular velocity of the rollers, with proportionality constant depending on device properties (its dimensions, roughness of rollers, fluid viscosity) [44]. Suppose, moreover, that it was desired to maintain the perturbed hyperbolic trajectory at a specified location $\mathbf{a}_\varepsilon(t) = \varepsilon\,(x_1(t), y_1(t))$, by introducing a perturbation to (5.1) in the form

$$\begin{pmatrix} \dot{x} \\ \dot{y} \end{pmatrix} = \begin{pmatrix} -\gamma x \\ \gamma y \end{pmatrix} + \varepsilon \mathbf{v}_1\,(x, y, t)\,. \tag{5.2}$$

Here, $\mathbf{a} = (0,0)$, $\lambda_u = -\lambda_s = \gamma$, $\mathbf{s} = -\hat{\mathbf{i}}$, $\mathbf{u} = \hat{\mathbf{j}}$, $\mathbf{s}^\perp = -\hat{\mathbf{j}}$, and $\mathbf{u}^\perp = -\hat{\mathbf{i}}$. From (2.6), $\tilde{\alpha}_u(t) = -x_1(t)$ and $\tilde{\alpha}_s(t) = y_1(t)$, and thus from (2.11), $\beta_u(t) = -x_1'(t) - \gamma x_1(t)$ and $\beta_s(t) = -y_1'(t) + \gamma y_1(t)$. Equation (2.10) gives the time-varying velocity required at the origin as

$$\mathbf{v}_1\,(\mathbf{0}, t) = \left[x_1'(t) + \gamma x_1(t)\right]\hat{\mathbf{i}} + \left[y_1'(t) - \gamma y_1(t)\right]\hat{\mathbf{j}}\,. \tag{5.3}$$

This is the identical expression that one would get if using (3.3) directly, or by substituting $\mathbf{a}_\varepsilon(t)$ of this form into (5.2) and formally Taylor expanding. If we would like $(x_1(t), y_1(t))$ to equal $(\cos\omega t, \sin\omega t)$—i.e., the hyperbolic trajectory rotating at angular frequency ω—then we need

$$\mathbf{v}_1\,(\mathbf{0}, t) = \left(-\omega\sin\omega t + \gamma\cos\omega t\right)\hat{\mathbf{i}} + \left(\omega\cos\omega t - \gamma\sin\omega t\right)\hat{\mathbf{j}}\,. \tag{5.4}$$

While $\mathbf{v}_1$ only needs to be known at the origin, it shall be extended uniformly in the vicinity of the origin to test the theory. The result is shown in Figure 4, which compares the required time-variation of the hyperbolic trajectory with the actual hyperbolic trajectory of the system (5.1) perturbed according to the control strategy (5.4). Numerically computing hyperbolic trajectories requires a little care, and details are given in Appendix A. Figure 4 indicates that the agreement between the specified hyperbolic trajectory and the actual one is excellent even with the relatively large value of ε. This is not surprising since in this specific instance the governing differential equation is exactly solvable (it is linear and homogeneous). We next examine a nonuniform extension of (5.4) which is shown in Figure 5, while retaining the relatively large value $\varepsilon = 0.1$. In this case, our strategy does not fully succeed in ensuring that the hyperbolic trajectory exhibits the time-periodic behavior $\varepsilon\,(\cos\omega t, \sin\omega t)$. However, the hyperbolic trajectory periodically traverses a nearby orbit, and the error remains bounded.

As a second example, suppose it were required that we keep the hyperbolic trajectory on the line $y = kx$ (where k is a given constant), while remaining $\mathcal{O}(\varepsilon)$-close to the origin. Set $\mathbf{a}_\varepsilon(t) = \varepsilon\,(g(t), kg(t))$ for some $\mathcal{O}(\varepsilon^0)$ function g. From either (2.10) or (3.3), the required control is

$$\mathbf{v}_1\,(\mathbf{0}, t) = \left(g'(t) + \gamma g(t)\right)\hat{\mathbf{i}} + k\left(g'(t) - \gamma g(t)\right)\hat{\mathbf{j}}\,. \tag{5.5}$$

Note that the hyperbolic trajectory can be moved to a *steady* location on the line $y = kx$ by choosing $g(t) =$ constant, for which $\mathbf{v}_1$ at the origin is seen to be in the

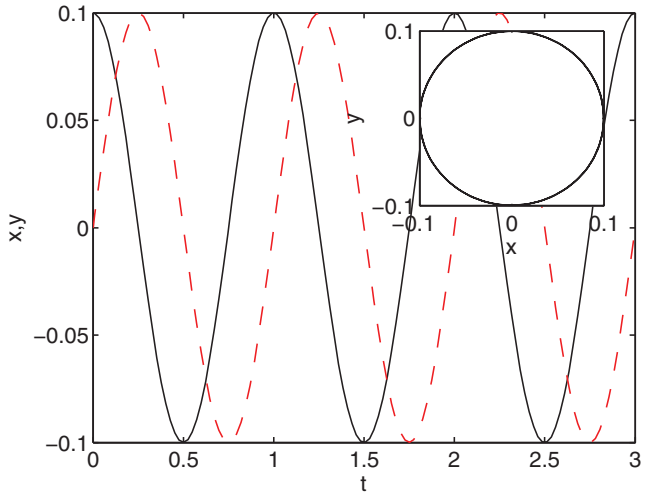

FIG. 4. *Numerically computed hyperbolic trajectory in the four-roll mill with uniform perturbation* (5.4)*, with* $\varepsilon = 0.1$*,* $\omega = 2\pi$*, and* $\gamma = 1$*. As desired, we obtain* $(x(t), y(t)) = \varepsilon(\cos\omega t, \sin\omega t)$*. The temporal evolution of* $x(t)$ *(solid) and* $y(t)$ *(dashed) is shown. The inset displays the trajectory in phase space* ($x(t)$ *vs* $y(t)$)*.*

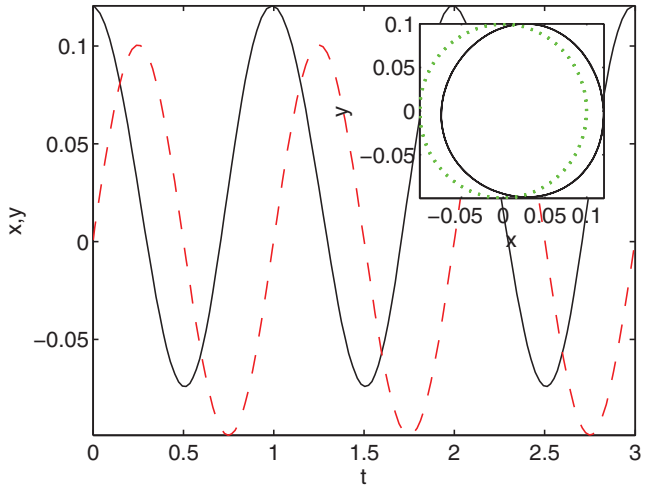

FIG. 5. *Numerically computed hyperbolic trajectory in the four-roll mill with nonuniform perturbation* $\mathbf{v}_1(x, y, t) = (-\omega \sin\omega t + \gamma \cos\omega t)(1 - x)(1 - y)\hat{\mathbf{i}} + (\omega \cos\omega t - \gamma \sin\omega t) \cos x\hat{\mathbf{j}}$*, which is consistent with* (5.4)*. Here,* $\varepsilon = 0.1$*,* $\omega = 2\pi$*, and* $\gamma = 1$*. The hyperbolic trajectory follows closely* $\varepsilon(\cos\omega t, \sin\omega t)$ *and exhibits time-periodic behavior. The inset shows the computed trajectory in phase space (solid) and desired motion (dotted).*

direction $\hat{\mathbf{i}} - k\hat{\mathbf{j}}$, which is *not* along the line $y = kx$, as might have been naively guessed. This illustrates the nonintuitive nature of the connection between the location of the hyperbolic trajectory and the Eulerian velocity. We choose a nonuniform extension of (5.5) to be

$$\mathbf{v}_1(x, y, t) = (g'(t) + \gamma g(t))\,(1 - x)(1 - y)\hat{\mathbf{i}} + k\,(g'(t) - \gamma g(t))\cosh x\hat{\mathbf{j}}\,, \tag{5.6}$$

and in Figure 6 we display the numerically obtained hyperbolic trajectory for a specific

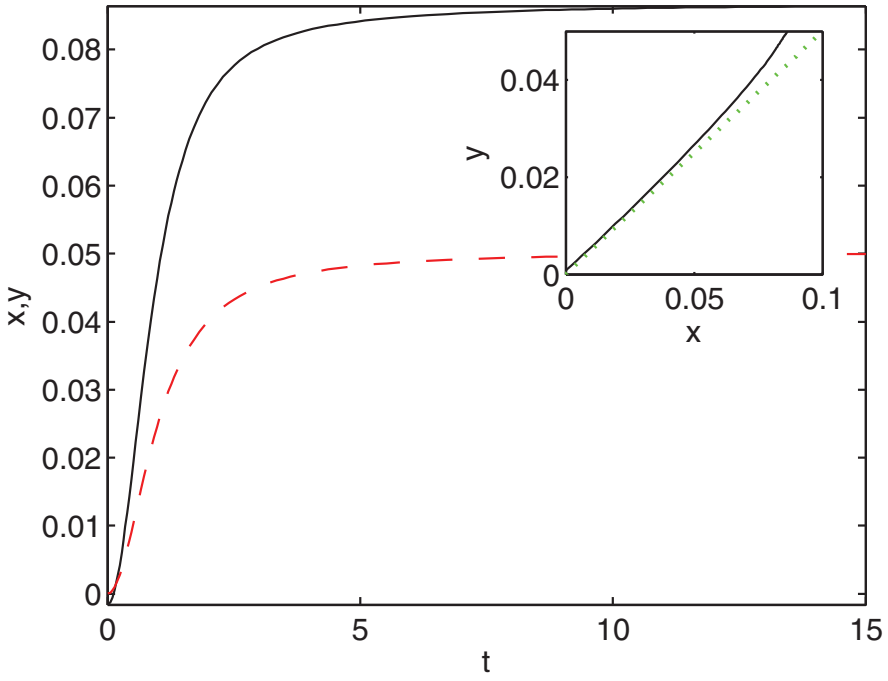

FIG. 6. *Numerically computed hyperbolic trajectory of the four-roll mill with the control Eulerian velocity* (5.6) *with the choice* $g(t) = t^2/(1+t^2)$, $k = 0.5$, $\gamma = 1$, *and* $\varepsilon = 0.1$. *In the inset one sees a growing deviation from the desired motion (dotted) to the actual trajectory (solid).*

choice of g. As before, the control strategy performs well, but in this case there is a growing deviation from the desired location.

We now analyze the error in the hyperbolic trajectory in comparison to our derived error bound (3.7). In this case, since $D\mathbf{v}_1(\mathbf{a})$ is not the zero matrix, the leading-order error term in (3.4) is nonzero. To verify the error bound as given in (3.7), we explicitly compute

$$|\mathbf{E}(t,\varepsilon)| \leq \varepsilon^2 c \left\| e^{D\mathbf{v}_0(\mathbf{a})t} - I \right\| = \varepsilon^2 c \left[2\cosh(\gamma t) - 1 \right], \tag{5.7}$$

which is valid for suitably small ε. In Figure 7, we investigate the time-variation of the error associated with the nonuniform control (5.6), in comparison to (5.7). The theoretical error bound works but is not necessarily very sharp.

6. Duffing oscillator. A frequently considered mechanical oscillator is the Duffing oscillator [18], which in the damped unforced situation has the form

$$\ddot{x} + \delta\dot{x} - x + x^3 = 0, \tag{6.1}$$

with $\delta > 0$ representing the damping coefficient. When expressed as a first-order system in the $(x, \dot{x})$ phase-space, this possesses a saddle $\mathbf{a} \equiv (0,0)$ and two attracting fixed points at $\mathbf{b}_1 \equiv (-1,0)$ and $\mathbf{b}_2 \equiv (1,0)$. The stable and unstable manifolds of $\mathbf{a}$ form boundaries of the basins of attraction of $\mathbf{b}_{1,2}$, and thus their location has important consequences for the resulting motion; see Figure 8. Now we consider

$$\ddot{x} + \delta\dot{x} - x + x^3 = \varepsilon f(x, \dot{x}, t), \tag{6.2}$$

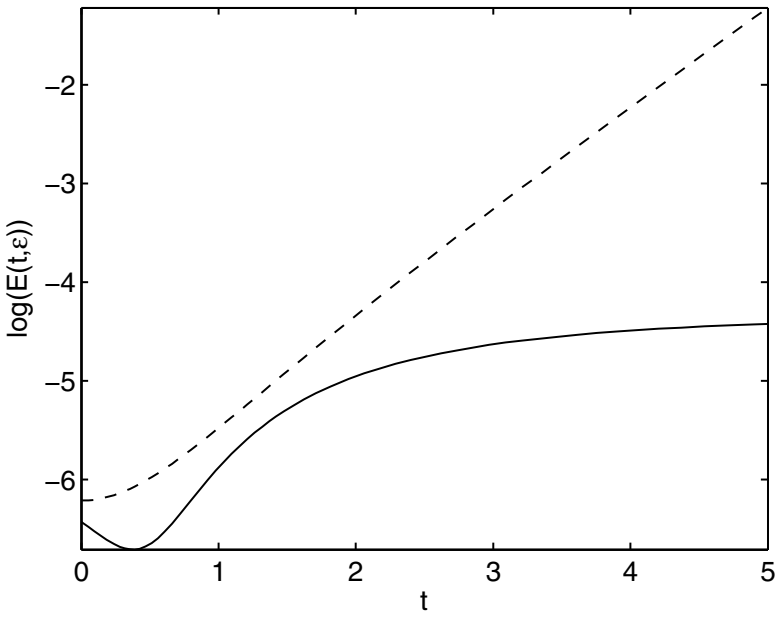

FIG. 7. *The time-growth of the error associated with the nonuniform control velocity* (5.6)*, with* $g(t) = t^2/(1+t^2)$*,* $k = 0.5$*, and* $\varepsilon = 0.1$*. The actual error (solid curve) is compared with the dashed error bound* (5.7)*, sketched here with* $c = 0.2$*.*

in which $|\varepsilon| \ll 1$ and the perturbative function f may depend on the position x, the velocity $\dot{x}$, or on time in any bounded way, thereby potentially modeling nonlinearities in the spring force and in damping in addition to arbitrary time-dependent forcing. The saddle perturbs to a time-varying hyperbolic trajectory $\mathbf{a}_\varepsilon(t)$ whose manifolds continue to demarcate basin boundaries, and thus controlling the location of $\mathbf{a}_\varepsilon(t)$ has important consequences on the dynamics. The system can be written as

$$\left.\begin{aligned} \dot{x} &= y, \\ \dot{y} &= x - x^3 - \delta y - \varepsilon f(x, y, t). \end{aligned}\right\} \tag{6.3}$$

Suppose that we need to maintain the hyperbolic trajectory at a location $\mathbf{a}_\varepsilon(t) = \varepsilon\,(x_1(t), y_1(t))$, where, in contrast to the previous example, $y_1(t) = \dot{x}_1(t)$ is automatically determined by (6.3). Thus, the control strategy can be obtained purely in terms of $x_1(t)$.

Now for (6.3) with $\varepsilon = 0$, $\mathbf{a} = \mathbf{0}$, $\lambda_s = (-\delta - \sqrt{4+\delta^2})/2$, $\lambda_u = (-\delta + \sqrt{4+\delta^2})/2$,

$$\mathbf{s} = \frac{1}{\sqrt{4 + \left(\delta - \sqrt{4+\delta^2}\right)^2}} \begin{pmatrix} \delta - \sqrt{4+\delta^2} \\ 2 \end{pmatrix},$$

$$\mathbf{u} = \frac{1}{\sqrt{4 + \left(\delta + \sqrt{4+\delta^2}\right)^2}} \begin{pmatrix} \delta + \sqrt{4+\delta^2} \\ 2 \end{pmatrix},$$

$$\mathbf{s}^\perp = \frac{1}{\sqrt{4 + \left(\delta - \sqrt{4+\delta^2}\right)^2}} \begin{pmatrix} -2 \\ \delta - \sqrt{4+\delta^2} \end{pmatrix},$$

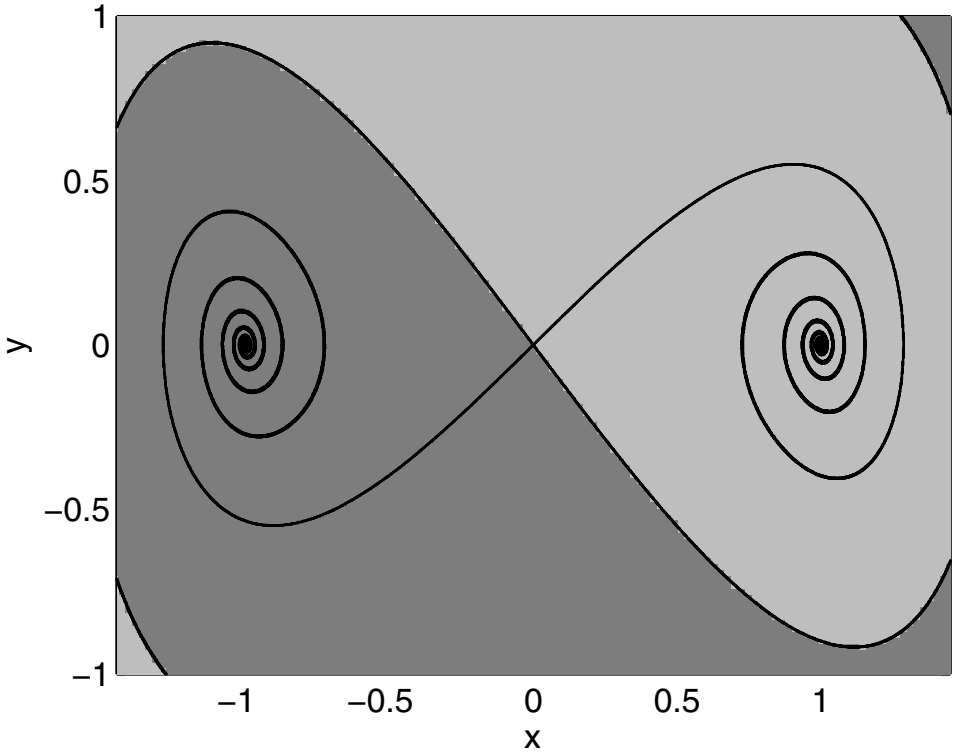

FIG. 8. *The phase space for the damped unforced Duffing oscillator* (6.1) *with* $\delta = 0.3$. *The shading represents the basins of attractions of the two attracting points* $(\pm 1, 0)$.

$$\mathbf{u}^{\perp} = \frac{1}{\sqrt{4 + \left(\delta + \sqrt{4+\delta^2}\right)^2}} \begin{pmatrix} -2 \\ \delta + \sqrt{4+\delta^2} \end{pmatrix}.$$

Calculating (2.6) and (2.11) gives complicated expressions, but when finally evaluating (2.10), many simplifications occur, and we get

$$\mathbf{v}_1(0,0,t) = \begin{pmatrix} 0 \\ \ddot{x_1}(t) + \delta \dot{x_1}(t) - x_1(t) \end{pmatrix}. \tag{6.4}$$

This needs to be consistent with the requirement from (6.3) that $\mathbf{v}_1(0,0,t)$ have components $(0, -f(0,0,t))$. Thus we arrive at the control condition

$$f(0,0,t) = -\ddot{x_1}(t) - \delta \dot{x_1}(t) + x_1(t) \tag{6.5}$$

on the perturbing function. We note that the process leading to the heuristically derived control formula (3.3) would lead to this expression very quickly by formal Taylor expansions, thereby verifying the equivalence of (2.10) and (3.3) in this instance as well. If one thinks of f as a purely forcing function, then (6.5) tells us how to force the oscillator in order to have approximately the hyperbolic response $\varepsilon x_1(t)$.

If, for example, $x_1(t) = \cos \omega t$ were required, then

$$f(0,0,t) = -\left(1+\omega^2\right)\cos(\omega t) - \delta\omega \sin(\omega t) = A(\omega)\cos(\omega t + \phi(\omega)), \tag{6.6}$$

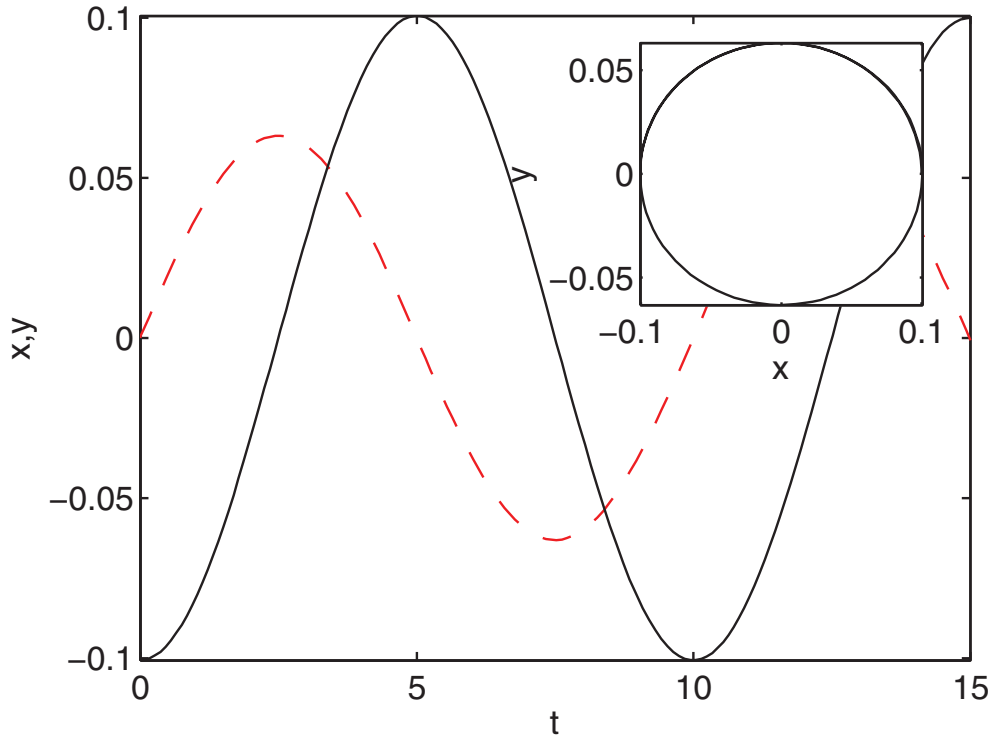

FIG. 9. *Numerically obtained hyperbolic trajectory of the damped Duffing oscillator* (6.3)*, with the control strategy* (6.6) *which is extended uniformly in* (x, y)*, and with* $\varepsilon = 0.1$*,* $\delta = 0.3$*, and* $\omega = 0.2\pi$*. The inset displays the trajectory in phase space.*

where the amplitude and phase angle are, respectively, $A(\omega) = \sqrt{\left(1+\omega^2\right)^2 + \delta^2\omega^2}$ and $\phi(\omega) = \sin^{-1}\left(\delta\omega/A(\omega)\right)$. As is well known, such systems have chaotic oscillations [18, 28, 27, 25, 45, 8], with the behavior (transferring between the two potential wells of (6.2) chaotically, exhibiting chaotic oscillations within one of the wells, etc.) being extremely sensitive to initial conditions chosen near the hyperbolic trajectory. Our control mechanism has provided a method for maintaining this crucial trajectory at a location of our choosing and, moreover, quantifies precisely the frequency-dependence on the phase difference between the imposed forcing and the response. The amplitude ratio between these quantities is also explicitly given by $A(\omega)$. Figure 9 displays the numerically obtained hyperbolic trajectory using the uniformly extended control forcing (6.6), exhibiting once again near-perfect performance even with $\varepsilon = 0.1$. For details on finding the hyperbolic trajectory numerically, we once again refer the reader to Appendix A.

We note that the multiplicative constant (3.6) in the error bound (3.4) is zero in this case, since all components of $D^2\mathbf{v}_0(\mathbf{a})$ and $D\mathbf{v}_1(\mathbf{a})$ are zero. A different example is needed to numerically investigate our error bound, and so we nonuniformly extend the control strategy (6.5) to

$$f(x, y, t) = [-\ddot{x}_1(t) - \delta\dot{x}_1(t) + x_1(t)]\cosh x\,, \tag{6.7}$$

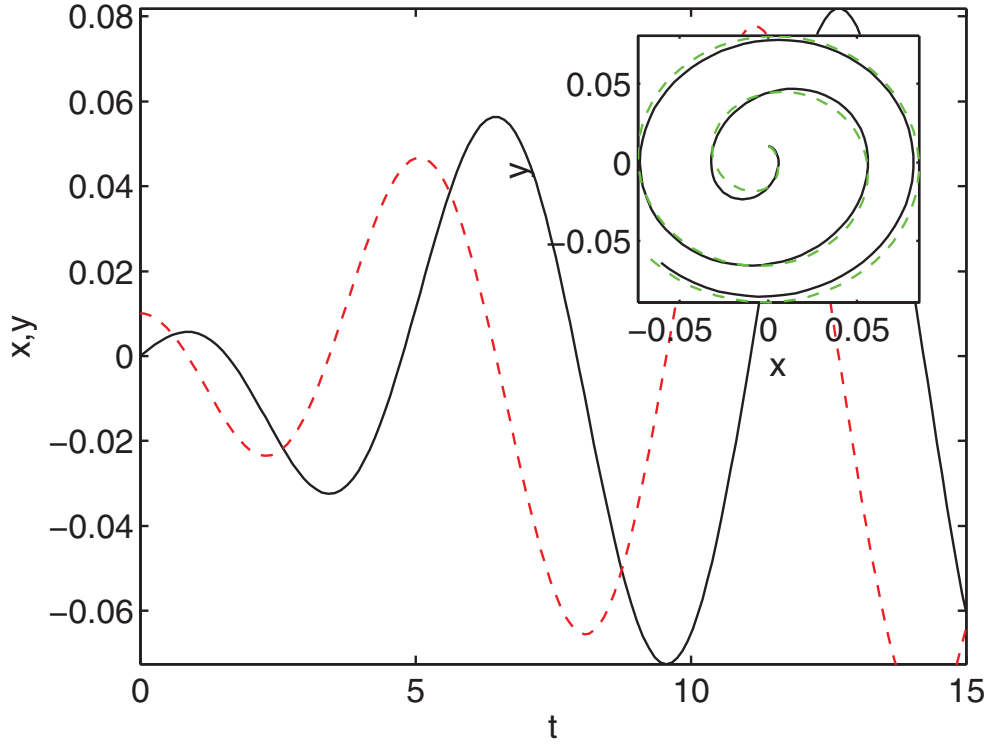

FIG. 10. *Numerically obtained hyperbolic trajectory of the damped Duffing oscillator* (6.3)*, with the nonuniform control strategy* (6.7) *and the desired trajectory* $x_1(t) = \cos t \tanh t/10$*, with* $\varepsilon = 0.1$ *and* $\delta = 0.3$*. In the inset one sees a growing deviation from the desired motion (dashed) to the actual trajectory (solid).*

which ensures that $D\mathbf{v}_1$ is no longer zero. We show in Figure 10 the result of applying this control strategy in attempting to achieve $x_1(t) = \cos t \tanh t/10$. Now, from (3.7), we explicitly get the error bound

$$\|\mathbf{E}(t,\varepsilon)| \leq \left\| e^{D\mathbf{v}_0(\mathbf{a})t} - I \right\| = \varepsilon^2 c e^t \tag{6.8}$$

for suitably small ε. We illustrate in Figure 11 the fact that the actual computed error in the hyperbolic trajectory obeys this theoretical bound.

7. Concluding remarks. In this article, we have established the velocity perturbation necessary to maintain a hyperbolic trajectory at a user-specified location. We verify that formula (3.3), which can be obtained quickly by formal Taylor expansion, is equivalent to (2.10), which we derived by appealing to previous results [4] on locating stable and unstable manifolds. The analysis does require that the flow be nearly steady, but, as shown in our four-roll mill and Duffing oscillator examples, the performance of the control strategy is excellent even when the unsteady velocity is as large as 10% of the base flow. We also provided an estimate on the time variation of the error in the hyperbolic trajectory as a result of a given control strategy and verified its accuracy in our examples. Controlling time-varying hyperbolic trajectories in this form has strong influence on nearby fluid transport (if a fluid mechanical

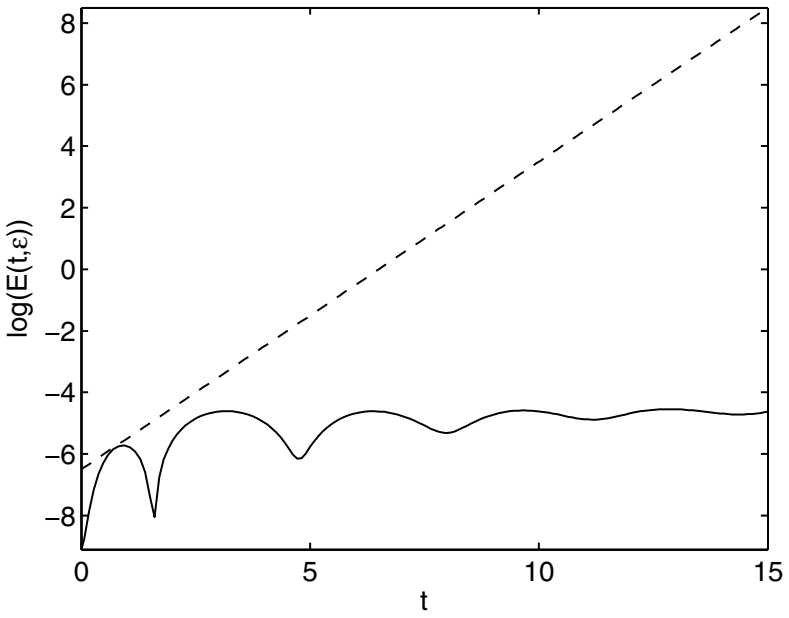

FIG. 11. *The time-growth of the error associated with the nonuniform control* (6.7)*, with* $x_1(t) = \cos t \tanh t/10$*,* $\varepsilon = 0.1$*, and* $\delta = 0.3$*. The actual error (solid curve) is compared with the dashed error bound* (6.8)*, sketched here with* $c = 0.15$*.*

system) or on basin boundaries demarcating different asymptotic fates (if a more general system), and thus knowing how to control these entities is important. In both these instances, it is the stable and unstable manifolds associated with the hyperbolic trajectories which are the important flow separators, and the next step would be to determine a control strategy which can keep these manifolds at specified time-varying locations. We address this inevitably more complicated issue in a subsequent article.

Appendix A. Computing hyperbolic trajectories numerically. In our special two-dimensional setting we are interested in solutions to driven ordinary differential equations that are both hyperbolic and bounded. Haller [19] derives an analytical criterion to find trajectories that are (uniformly) hyperbolic on a given time span $I \subset \mathbb{R}$: given a sufficiently smooth two-dimensional velocity field in the form of (2.1), a necessary condition for a solution $\mathbf{x}(t)$ to be finite-time hyperbolic on I is that $\det D_{\mathbf{x}}\mathbf{v}\,(\mathbf{x}(t), t) < 0$ for all $t \in I$. If, as in our example systems, the associated finite-time stable and unstable manifolds do not change very fast (measured in terms of the rate of change of a matrix containing the corresponding tangent vectors), the determinant condition also becomes sufficient. Note, in particular, that by a spatially uniform time-dependent forcing the respective stable and unstable manifolds are only translated in space, resulting in a constant matrix of tangent vectors.

Unlike the Duffing system considered in section 6, in the four-roll mill example of section 5 the determinant criterion is useless. The reason is that a spatially uniform time-dependent forcing makes all trajectories uniformly hyperbolic. Hyperbolicity of the controlled trajectories in this linear instance can be easily verified analytically (see, e.g., section 2.1 in Ju, Small, and Wiggins [24]). Thus we just need to check that

these trajectories are the only bounded trajectories of the forced system, staying in an ε-neighborhood of the saddle stagnation point.

We exploit these ideas in a numerical scheme by adapting set-oriented methods for the approximation of invariant sets [12, 13]. For this we fix a certain time slice $t_0 \in \mathbb{R}$, a small flow time $T > 0$, and a neighborhood of the saddle stagnation point strictly containing the ε-neighborhood of interest. We form a partition of this neighborhood into small connected subsets and then follow a twofold approach: (i) we refine the partition by subdividing the partition elements into smaller subsets, and (ii) we discard those sets for which we cannot find a valid initial condition in the set. By a valid initial condition we mean one whose trajectory satisfies the determinant and boundedness criteria in both forwards (i.e., on $[t_0, t_0 + T]$) and backwards ($[t_0 - T, t_0]$) time. For the selection step (ii) appropriate test point strategies are employed, which could also be made rigorous following the ideas of Dellnitz and Junge [13]. We alternate steps (i) and (ii) while increasing T until we have obtained a tight bound on the initial conditions that give rise to hyperbolic trajectories. In our examples here, this allows us to pinpoint the initial conditions of hyperbolic trajectories up to an accuracy on the order of 10^{-8}. We note that this approach is independent of the nature of the perturbations and, unlike the study of Poincaré return maps, is not restricted to time-periodic forcings.

REFERENCES

[1] B. Aldridge, G. Haller, P. Sorger, and D. Lauffenburger, *Direct Lyapunov exponent analysis enables parametric study of transient signaling governing cell behaviour*, Syst. Biol., 153 (2006), pp. 425–432.

[2] F. Arai, A. Ichikawa, T. Fukuda, K. Horio, and K. Itoigawa, *Stagnation point control by pressure balancing in microchannel for high speed and high purity separation of microobject*, in Proceedings of the 2001 IEEE/RSJ International Conference on Intelligent Robots and Systems, 2001, pp. 1343–1348.

[3] S. Balasuriya, *Gradient evolution for potential vorticity flows*, Nonlinear Proc. Geophys., 8 (2001), pp. 253–263.

[4] S. Balasuriya, *A tangential displacement theory for locating perturbed saddles and their manifolds*, SIAM J. Appl. Dyn. Syst., 10 (2011), pp. 1100–1126.

[5] S. Balasuriya, *Explicit invariant manifolds and specialised trajectories in a class of unsteady flows*, Phys. Fluids, 24 (2012), 12710.

[6] B. Bentley and L. Leal, *A computer-controlled four-roll mill for investigations of particle and drop dynamics in two-dimensional shear flows*, J. Fluid Mech., 167 (1986), pp. 219–240.

[7] Z. Bishnani and R. MacKay, *Safety criteria for aperiodically forced systems*, Dynamical Systems, 18 (2003), pp. 107–129.

[8] E. Bollt, *Combinatorial control of global dynamics in a chaotic differential equation*, Internat. J. Bifurc. Control, 11 (2001), pp. 2145–2162.

[9] M. Branicki, A. Mancho, and S. Wiggins, *A Lagrangian description of transport associated with front-eddy interaction: Application to data from the North-Western Mediterranean Sea*, Phys. D, 240 (2011), pp. 282–304.

[10] W. A. Coppel, *Dichotomies in Stability Theory*, Lecture Notes in Math. 629, Springer-Verlag, Berlin, 1978.

[11] D. del Castillo Negrete and P. Morrison, *Chaotic transport by Rossby waves in shear flow*, Phys. Fluids A, 5 (1993), pp. 948–965.

[12] M. Dellnitz and A. Hohmann, *A subdivision algorithm for the computation of unstable manifolds and global attractors*, Numer. Math., 75 (1997), pp. 293–317.

[13] M. Dellnitz and O. Junge, *Set oriented numerical methods for dynamical systems*, in Handbook of Dynamical Systems 2, Elsevier Science, New York, 2002, pp. 221–264.

[14] K. El Rifai, G. Haller, and A. Bajaj, *Global dynamics of an autoparametric spring-mass-pendulum system*, Nonlinear Dynam., 49 (2007), pp. 105–116.

[15] A. Fradkov, R. Evans, and B. Andrievsky, *Control of chaos: Methods and applications in mechanics*, Phil. Trans. Roy. Soc. A, 364 (2006), pp. 2279–2307.

[16] A. L. Fradkov and R. J. Evans, *Control of chaos: Methods and applications in engineering*, Annu. Rev. Control, 29 (2005), pp. 33–56.
[17] P. Gaskell, M. Savage, and H. Thompson, *Stagnation-saddle points and flow patterns in Stokes flow between contra-rotating cylinders*, J. Fluid Mech., 370 (1998), pp. 221–247.
[18] J. Guckenheimer and P. Holmes, *Nonlinear Oscillations, Dynamical Systems and Bifurcations of Vector Fields*, Springer, New York, 1983.
[19] G. Haller, *Finding finite-time invariant manifolds in two-dimensional velocity fields*, Chaos, 10 (2000), pp. 99–108.
[20] G. Haller and A. Poje, *Finite time transport in aperiodic flows*, Phys. D, 119 (1998), pp. 352–380.
[21] S. Hu, D. LaCroix, and A. McFarland, *Stagnation point displacement: Control of losses on a conically shaped aerosol distributor*, Aerosol Sci. Tech., 43 (2009), pp. 311–321.
[22] Y. Hu, D. Pine, and L. Leal, *Drop deformation, breakup, and coalescence with compatibilizer*, Phys. Fluids, 12 (2000), pp. 484–489.
[23] S. Hudson, F. Phelan, M. Handler, J. Cabral, K. Migler, and E. Amis, *Microfluidic analog of the four-roll mill*, Appl. Phys. Lett., 85 (2004), pp. 335–337.
[24] N. Ju, D. Small, and S. Wiggins, *Existence and computation of hyperbolic trajectories of aperiodically time dependent vector fields and their approximations*, Internat. J. Bifur. Chaos Appl. Sci. Engrg., 13 (2003), pp. 1449–1457.
[25] A. Katz and E. Dowell, *From single-well chaos to cross-well chaos: A detailed explanation in terms of manifold intersections*, Internat. J. Bifur. Chaos Appl. Sci. Engrg., 4 (1994), pp. 933–941.
[26] J. Lee, R. Dylla-Spears, N. Teclemariam, and S. Muller, *Microfluidic four-roll mill for all flow types*, Appl. Phys. Lett., 90 (2007), 074103.
[27] S. Lenci and G. Rega, *Optimal numerical control of single-well to cross-well chaos transition in mechanical systems*, Chaos Solitons Fractals, 15 (2003), pp. 173–186.
[28] R. Lima and M. Pettini, *Parametric resonant control of chaos*, Internat. J. Bifur. Chaos Appl. Sci. Engrg., 8 (1998), pp. 1675–1684.
[29] C. Lu, R. Gong, and J. Luo, *Analysis of stagnation points for a pumping well in recharge areas*, J. Hydrol., 373 (2009), pp. 442–452.
[30] K. Lu and Q. Wang, *Chaotic behavior in differential equations driven by a Brownian motion*, J. Differential Equations, 251 (2011), pp. 2853–2895.
[31] O. Malaspinas, N. Fietier, and M. Deville, *Lattice Boltzmann method for the simulation of viscoelastic fluid flows*, J. Non-Newtonian Fluid Mech., 165 (2010), pp. 1637–1653.
[32] A. Mancho, D. Small, S. Wiggins, and K. Ide, *Computation of stable and unstable manifolds of hyperbolic trajectories in two-dimensional, aperiodically time-dependent vector fields*, Phys. D, 182 (2003), pp. 188–222.
[33] E. Ott, C. Grebogi, and J. A. Yorke, *Controlling chaos*, Phys. Rev. Lett., 64 (1990), pp. 1196–1199.
[34] K. Padberg, T. Hauff, F. Jenko, and O. Junge, *Lagrangian structures and transport in turbulent magnetized plasmas*, New J. Phys, 9 (2007), 400.
[35] K. Palmer, *Exponential dichotomies and transversal homoclinic points*, J. Differential Equations, 55 (1984), pp. 225–256.
[36] R. Pierrehumbert, *Chaotic mixing of tracer and vorticity by modulated travelling Rossby waves*, Geophys. Astrophys. Fluid Dyn., 58 (1991), pp. 285–319.
[37] K. Pyragas, *Continuous control of chaos by self-controlling feedback*, Phys. Lett. A, 170 (1992), pp. 421–428.
[38] V. Rom-Kedar, A. Leonard, and S. Wiggins, *An analytical study of transport, mixing and chaos in an unsteady vortical flow*, J. Fluid Mech., 214 (1990), pp. 347–394.
[39] S. Ross, M. Tanaka, and C. Senatore, *Detecting dynamical boundaries from kinematic data in biomechanics*, Chaos, 20 (2010), 017507.
[40] I. Rypina, M. Brown, and H. Koçak, *Transport in an idealized three-gyre system with applications to the Adriatic Sea*, J. Phys. Oceanogr., 39 (2009), pp. 675–690.
[41] R. Sacker and G. Sell, *The spectrum of an invariant submanifold*, J. Differential Equations, 38 (1980), pp. 135–160.
[42] J. Soulages, M. Oliveira, P. Souza, M. Alves, and G. H. McKinley, *Investigating the stability of viscoelastic stagnation flows in T-shaped microchannels*, J. Non-Newtonian Fluid Mech., 163 (2009), pp. 9–24.
[43] A. Szeri, W. Milliken, and L. Leal, *Rigid particles suspended in time-dependent flows—Irregular versus regular motion, disorder versus order*, J. Fluid Mech., 237 (2006), pp. 33–56.
[44] G. Taylor, *The formation of emulsions in definable fields of flow*, Proc. R. Soc. London Ser. A, 146 (1934), pp. 501–523.

[45] Y. Ueda, S. Yoshida, and H. B. Stewart, and J. M. T. Thompson, *Basin explosions and escape phenomena in the twin-well Duffing oscillator: Compound global bifurcations organizing behaviour*, Phil. Trans. Roy. Soc. London Ser. A, 332 (1990), pp. 169–186.

[46] O. A. van Herwaarden, *Spread of pollution by dispersive groundwater flow*, SIAM J. Appl. Math., 54 (1994), pp. 26–41.

[47] S. Wereley and S. Gui, *A correlation-based central difference image correction (CDIC) method and application in a four-roll mill flow PIV measurement*, Exper. Fluids, 34 (2003), pp. 42–51.

[48] J. Whitehead, *Topographic control of oceanic flows in deep passages and straits*, Rev. Geophys., 36 (1998), pp. 423–440.

[49] J. Wintersmith, L. Zou, A. Bernoff, J. Alexander, J. Mann, E. Kooijman, and E. Mann, *Determination of interphase line tension in Langmuir films*, Phys. Rev. E, 75 (2007), 061605.

[50] W. Xu and S. Muller, *Exploring both sequence detection and restriction endonuclease cleavage kinetics by recognition site via single-molecule microfluidic trapping*, Lab Chip, 11 (2011), pp. 435–442.

[51] K. Yagasaki, *Invariant manifolds and control of hyperbolic trajectories on infinite- or finite-time intervals*, Dynam. Systems, 23 (2008), pp. 309–331.

[52] J. Yang and Y. Xu, *Coalescence of two viscoelastic droplets connected by a string*, Phys. Fluids, 20 (2008), 043101.

[53] Y. Yi, *A generalized integral manifold theorem*, J. Differential Equations, 102 (1993), pp. 153–187.